Graphene oxide foils as osteoinductive stem cells substrate

Journal:	*ACS Applied Bio Materials*
Manuscript ID	mt-2019-000414.R2
Manuscript Type:	Article
Date Submitted by the Author:	n/a
Complete List of Authors:	Di Crescenzo, Antonello; Gabriele d'Annunzio University of Chieti and Pescara, Department of Pharmacy Zara, Susi; Gabriele d'Annunzio University of Chieti and Pescara, Department of Pharmacy Di Nisio, Chiara; Gabriele d'Annunzio University of Chieti and Pescara, Department of Pharmacy Ettorre, Valeria; Gabriele d'Annunzio University of Chieti and Pescara, Department of Pharmacy Ventrella, Alessia; Universita degli Studi Gabriele d'Annunzio Chieti e Pescara, Department of Pharmacy Zavan, Barbara; University of Padua, Department of Biomedical Sciences Di Profio, Pietro; Universita degli Studi Gabriele d'Annunzio Chieti e Pescara, Dipartimento di Farmacia Cataldi, Amelia; Gabriele d'Annunzio University of Chieti and Pescara, Department of Pharmacy Fontana, Antonella; Gabriele d'Annunzio University of Chieti and Pescara, Department of Pharmacy

Graphene oxide foils as osteoinductive stem cells substrate

Antonello Di Crescenzo,[‡, 1] *Susi Zara,*[‡, 1] *Chiara Di Nisio,*[1] *Valeria Ettorre,*[1] *Alessia Ventrella,*[1] *Barbara Zavan,*[2] *Pietro Di Profio,*[1] *Amelia Cataldi,*[1] *Antonella Fontana**[, 1]

[1] Dipartimento di Farmacia, University "G. d'Annunzio", Via dei Vestini, I-66100 Chieti, Italy.

[2] Dipartimento di Scienze Biomediche, University of Padova, Via Ugo Bassi, 58/B, I-35121 Padova, Italy.

Corresponding Author: fontana@unich.it (AF)

KEY WORDS: Graphene oxide, graphene oxide foil, atomic force microscopy, stem cells, osteoinductivity

‡These authors contributed equally.

ABSTRACT. The hydrophilic graphene derivative, graphene oxide (GO), is used to synthesize free-standing GO foils characterized by cross-linked GO sheets with enhanced mechanical properties and no tendency to release GO flakes in aqueous solution. These GO foils do not evidence cytotoxic effects towards Dental Pulp Stem Cells (DPSC). Rather, DPSC viability is

significantly increased for cells grown on GO foil and SEM analyses evidence the synthesis of consistent extracellular matrix by DPSCs with respect to cells grown on polystyrene. Gene expression of osteogenic markers and alkaline phosphatase (ALP) activity tests demonstrate DPSC differentiation towards the osteoblastic lineage. Indeed RUNX2, a key transcriptor factor associated with osteogenic differentiation, as well as SP7, responsible for triggering bone matrix mineralization, are significantly augmented after 7 and 14 days of culture on GO foil with respect to the control, respectively, underlying the capability of GO foil to promote a potential faster and better DPSC differentiation with respect to cells grown on polystyrene. This increase of rate differentiation is confirmed by SEM analyses of DPSCs evidencing a consistent extracellular matrix synthesis at the earliest time of culture (i.e. 3 and 14 days).

1. INTRODUCTION

Graphene oxide (GO) has received increasing attention among researchers due to the ability to disclose some of the exceptional features of pristine graphene[1-3] as well as the capacity to be well dispersed in both water[4,5] and organic solvents.[6] As a matter of fact graphene oxide resembles graphene because it is a single layer thick molecule combining honeycomb-structured aromatic carbon atom regions of unoxidized benzene rings and regions with oxygen-functionalized carbon atoms.[7] Indeed, differently from pure graphene, GO contains oxygen atoms in moieties such as hydroxyl, epoxy, carbonyl and carboxyl groups that decorate both its basal planes and edges.[4,7,8] These functional groups confer graphene oxide properties that pristine graphene lacks. In particular, the presence of these functionalities allows to easily keep GO well exfoliated in solution and favors its chemical modification with other functionalities. Furthermore, the carboxyl groups, as well as the enolizable keto groups, can act as proton donors making GO

acidic[4] and able to exchange hydrogen bonds with other GO sheets and water molecules. In addition, the presence of oxygen functional groups onto the graphene surface implies the possibility to exploit calcium ions as cross-linkers among GO sheets. Indeed, calcium and magnesium ions have been used to favor aggregation and consequent precipitation of GO sheets from relevant aqueous dispersions.[9] These properties should favor the formation of macroscopic foils of GO from the interconnection of GO sheet to each other via water molecules[10] and alkali-metals chelation.[9]

A large number of studies on GO has been stimulated for biomedical applications due to its demonstrated great osteoconductive and osteoinductive abilities for regulating osteoblastic differentiation,[11,12,13,14] as well as capacity to interact with cell membrane[15] and reported antimicrobial and antibiofilm efficacy.[16,17] Indeed, it has been demonstrated that stem cells undergo osteogenic differentiation in fetal bovine serum-containing medium without the addition of any glucocorticoid or specific growth factors.[18]

In the present study GO is used to synthesize GO foils characterized by cross-linked GO sheets that, aside from conferring to the paper remarkable mechanical properties,[9,19] demonstrate to improve GO biocompatibility and ability to induce Dental Pulp Stem Cells (DPSCs) differentiation towards the osteogenic/odontogenic lineage. Indeed, compared to previously published studies[5,20] on GO coatings or on graphene-based composites,[21,22] the present GO foils are free-standing micrometric 3D porous substrates made only of graphene oxide sheets hold together by interlamellar bonds via water molecules[10] and alkali-metals chelation.[9] This material offers a ready to use substrate characterized by an ideal Young's modulus, able to favor cell growth and adhesion without the drawback of GO leakage in the marrow spaces or in the soft tissues.

2. EXPERIMENTAL SECTION

2.1 Preparation of graphene oxide foils. A 3 mg/mL aqueous dispersion of GO sheets was prepared by dilution with milliQ water of commercially available (Graphenea, Donostia-San Sebastian, Spain) 4 mg/mL GO solution and subsequent bath ultrasonication for 10 minutes (Elmasonic P60H, 37 kHz, 180 W). The GO foil was prepared by vacuum-filtering 10 mL of the above dispersion through an Anodisc membrane filter (47 mm in diameter, 0.2 μm pore size, Whatman, Middlesex, U.K.) followed by addition of 10 mL of 0.2 mM $CaCl_2$ aqueous solution.[9] After the filtration, 10 mL of milliQ water was passed 3 times through the wet paper. The as-prepared Ca-modified GO foil was vacuum-dried for 24 h, then air-dried for 48 h and finally peeled from the filter (Figure 1). The GO paper was cut into small squares of size 5 × 5 mm to be subjected to investigations.

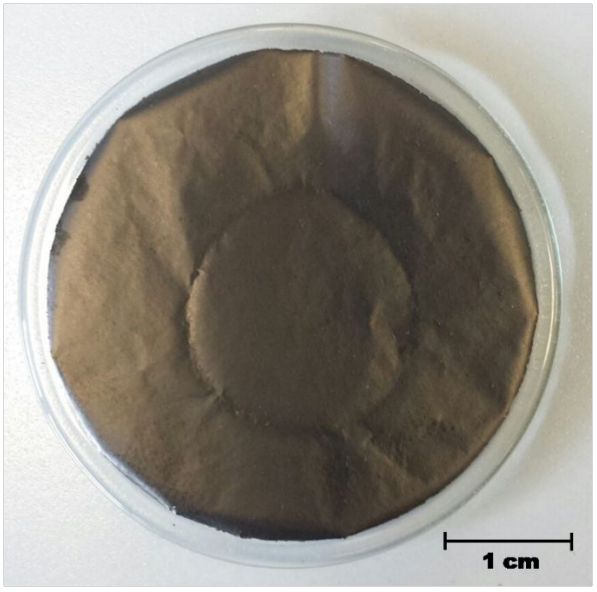

Figure 1. Photograph of a graphene oxide foil

2.2. Stability of the graphene oxide foil. Small pieces of GO foil were placed in 5 mL of milliQ water and in 5 mL of PBS and in both cases no evidence of dissolution was highlighted after one week (see Figure 2). Relevant UV-visible spectra of the aqueous solution before and after a week from contact with GO foil do not evidence GO leakage in the bulk water (see Supporting Information)

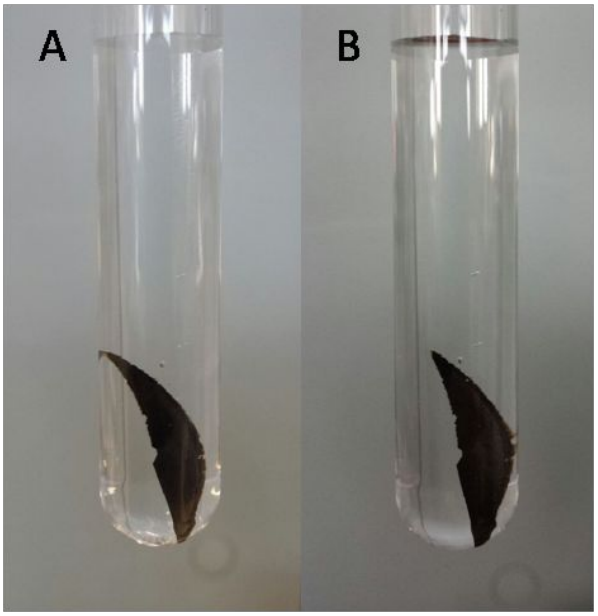

Figure 2. Graphene oxide foil in 5 mL of milliQ water (A) freshly prepared and (B) after 7 days.

2.3. AFM and SEM characterization. Atomic force microscopy analyses were obtained on a MultiMode 8, operating in Peak Force QNM mode, using a silicon cantilever equipped with a RTESPA-150 tip (spring constant = 5 N/m, resonant frequency =150 kHz). Peak Force QNM allowed to perform a quantitative nanomechanical evaluation of dissipation energy, deformation and adhesion across 10 μm × 10 μm sized area of each sample and to calculate the relevant Young's modulus. In particular, NanoScope Analysis software 1.5 enables to select the force curves registered at each point of the scanned surface and to calculate the Young's modulus by

fitting the retracting curve via hertzian model. The deflection sensitivity and tip radius were calibrated, prior to use, against standard sapphire. The specimen was prepared by laying a square of GO foil on the adhesive tape placed on the sampler puck. Scanning electron microscopy (SEM) was used to estimate the thickness of the GO foil from cross-section image acquired by a FEG SEM (ZEISS-GEMINI LEO 1530) at the 8 kV beam energy.

2.4. Sterilization of membranes. The sterilization of each scaffold was performed by UV irradiating the GO foils for 2 h. We checked that sterilization, performed under a germicide UV lamp (15 W), did not alter or reduce graphene oxide.[23,24] As a matter of fact no change of color, i.e. the appearance of a black area indicating GO reduction,[25] of the foil and no release of GO in water was observed. Indeed a reduction of GO was previously obtained by using a much higher lamp power (500 W).[25]

2.5. Cultivation of DPSCs. DPSCs were purchased from Lonza (Switzerland) and cultured in αMEM medium supplemented with 10% FBS and 1% penicillin/streptomycin. The medium was refreshed two times weekly to remove cells debris. When a sub-confluence condition was reached (80-90% of flask area), the cells were subcultured.

2.6. DPSCs cultivation on GO foils. DPSCs cultured up to four or five passages were used for the experiment. Cells were seeded on GO foils at 10000/cm^2 density and cultured up to 28 days. The cells were cultured using differentiation inducing medium (α-MEM, 10% FBS, 10nM dexamethasone, 0.2 mM ascorbic acid, 10mM β-glycerophosphate, 1% penicillin/streptavidin, DM) for 3, 7, 14, 21 and 28 days.

2.7. Scanning electron microscopy of DPSCs cultured on GO foils. Samples were fixed with 1.25% glutaraldehyde in 0.1 M cacodylate buffer for 30 min before processing with

hexamethyldisilazane followed by gold-palladium coating. All micrographs were obtained at 20 kV on a JEOL 6360LV SEM microscope (JEOL, Tokyo, Japan). The SEM analysis was carried out at the Interdepartmental Service Center C.U.G.A.S. (University of Padua).

2.8. Alamar blue cell viability assay. This assay was performed in triplicate for each experimental group at each time point. 3, 7, 14 and 28 days were chosen as experimental times to evaluate DPSCs viability. Alamar Blue test is based on the reduction of Alamar Blue reagent (resaruzin, 7-hydroxy-3H-phenoxazin-3-one 10-oxide) into a red product performed only by viable cells. At established experimental times the medium was removed and cells were probed with fresh medium supplemented with 10% of Alamar Blue reagent (Thermo Scientific, Rockford, IL, USA) for 4 h at 37°C. A spectrophotometric reading at 570 and 600 nm wavelength was performed after incubation. Negative control was assumed as the value obtained without cells. Alamar blue reagent % reduction was calculated according to the manufacturer's instruction.

2.9. Cytotoxicity assay (LDH assay). Membrane integrity of DPSCs was assessed by lactate dehydrogenase (LDH) leakage into the medium, quantified by using "CytoTox 96 non-radioactive cytotoxicity assay" (Promega, Madison, WI, USA), following the instruction of the manufacturer, after 3, 7, 14 and 28 days of culture on GO foil. LDH leakage obtained in each well was normalized to the % Alamar blue reduction value measured by the Alamar blue test.

2.10. RNA extraction. Total RNA was extracted with TRI Reagent (Sigma-Aldrich, St. Louis, MO, USA). Cells cultured on GO foil were treated with 500 μL of TRI Reagent to obtain a cell suspension. The latter was centrifuged at 10,000 rpm for 10 min at 4°C in order to eliminate insoluble material. 100 μL of chloroform were added to the supernatant under energetic mixing,

incubated on ice for 15 min and centrifuged for 20 min at 13,200 rpm at 4°C. The addition of 250 μL of isopropanol, storage for 30 min at −20°C and centrifugation at 13,200 rpm for 20 min at 4°C allowed to precipitate RNA in the aqueous phase. The RNA pellet was rinsed with 500 μL of 75% ethanol, air dried and then resuspended in RNase-free water. DNA-free kit (Life Technologies, Carlsbad, CA, USA) was used to remove contaminating DNA. A spectrophotometric reading at 260 nm wavelength was performed to evaluate RNA concentration; RNA purity was established considering the ratio of the absorbance measured at 260 wavelenght and that measured at 280 nm wavelength (BioPhotometer Eppendorf, Hamburg, Germany). The quality of extracted RNA was evaluated by performing electrophoresis with agarose gels and visualizing the sample under UV light after staining with ethidium bromide.

2.11. Reverse transcription (RT) and real-time RT-polymerase chain reaction (real-time RT-PCR). To reverse transcribe 1 μg of RNA a High Capacity cDNA Reverse Transcription kit (Life Technologies, Carlsbad, CA, USA) was applied in a reaction volume of 20 μL. Reactions were performed in a 2720 Thermal Cycler (Life Technologies) initially for 10 min at 25°C, then for 2 h at 37°C and eventually for 5 min at 85°C. Quantitative PCR was used to evaluate gene expression by means of TaqMan probe-based chemistry. Reactions were carried out in 96 multiwell plates on an ABI PRISM 7900 HT Fast Real-Time PCR System (Life Technologies, Carlsbad, CA, USA). TaqMan probes and PCR primers were purchased from Life Technologies (TaqMan Gene Expression Assays (20X): Hs00154192_m1 for BMP2, Hs00231692_m1 for RUNX2, Hs01866874_s1 for SP7). Glyceraldehyde-3-phosphate dehydrogenase (GAPDH) (Life Technologies, Part No. 4333764F, Carlsbad, CA, USA) was chosen as the housekeeping gene. The amplification reactions, performed at 95°C for 20 s, then at 95°C for 1 s for 40 cycles of amplification and afterwards at 60°C for 20 s, were carried out with 10 μL of TaqMan Fast

Universal PCR Master Mix (2X), No AmpErase UNG (Life Technologies, Carlsbad, CA, USA), 1 μL of primer-probe mixture, 1 μL of cDNA and 8 μL of nuclease-free water. To check contamination a no-template control was applied. For SP7 gene assay a reverse transcriptase minus control was added. Gene expression data were analyzed with Sequence Detection System software, version 2.3 (Life Technologies, Carlsbad, CA, USA). The relative abundance of mRNA was quantified by using the comparative $2^{-\Delta\Delta Ct}$ method (relative quantification). Real-time PCR analysis was carried out in five separate experiments. A cDNA sample was included in each experiment, for each experimental condition. Amplification was performed in triplicate for each cDNA sample in relation to each of the investigated genes. GraphPad Prism software, version 6.01, for Windows (GraphPad Software, San Diego, CA, USA) was used to evaluate statistical significance. Data were determined and expressed as means ± SEM for each experimental group. Values were analyzed by one-sample t-test. A gene expression value of 1 for the calibrator sample was considered the theoretical mean for the comparison. The level of statistical significance was set as $p<0.05$.

2.12. Alkaline Phosphatase activity. Alkaline phosphatase (ALP) catalyzes the hydrolysis of phosphate esters in alkaline buffer and produces an organic radical and inorganic phosphate. ALP activity was analyzed in cell supernatants using the Alkaline Phosphatase Assay Kit (Colorimetric) (Abcam, Cambridge, UK). The kit uses p-nitrophenyl phosphate (pNPP) as a phosphatase substrate which turns yellow (λ_{max}= 405 nm) when dephosphorylated by ALP. Cell supernatants were collected after 3, 7, 14, and 28 days of culture. After collection, 80 μL/well of sample were loaded in 96 Flat Bottom multiwell in duplicate. Next, 50 μL of pNPP 5 mM/well were added and the plate was incubated for 1 hour at room temperature in the dark. After that, 20 μL of stop solution were pipetted into each well and the absorbance output was measured at 405 nm by microplate

reader (Multiskan GO, Thermo Scientific, MA, USA). Each test was performed in triplicate ALP activity (U/L/min) was carried out following manufacturer's instructions and each value was normalized on the Alamar blue values.

3. RESULTS

3.1. GO foil characterization. GO foils have been previously extensively characterized in terms of tensile strength and interlamellar distance via X-ray diffraction.[9] We therefore performed Scanning electron microscopy (SEM) measurements in order to investigate the structure of GO inside the foil. SEM was used to estimate the thickness of the GO foil from cross-section. The GO foil, 10 μm thick, demonstrated to be formed by the superimposition of GO flakes one over the other (Figure 3).

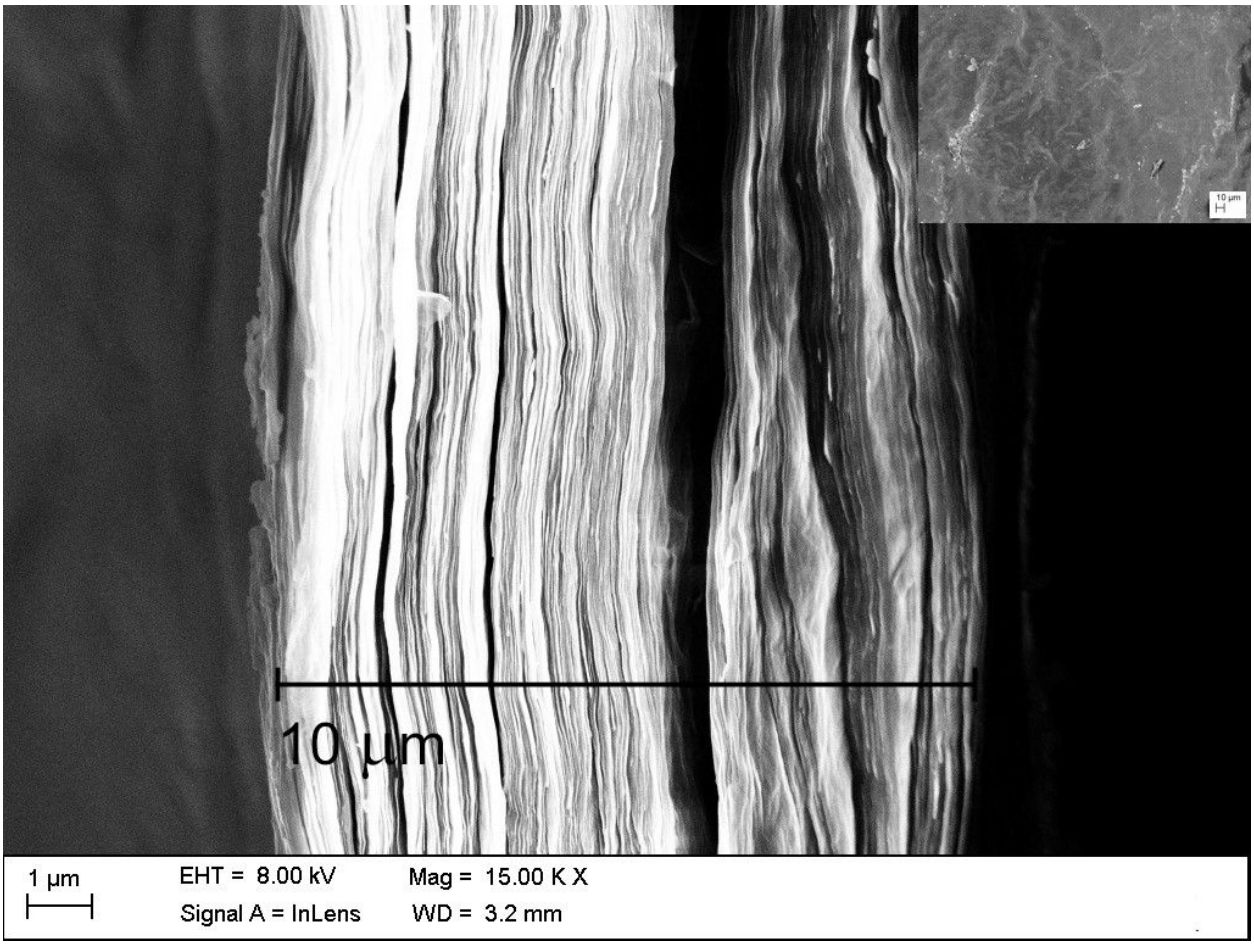

Figure 3. SEM micrographs of GO foil. The inset shows the surface of GO foil. This image has been performed at the Department of Physical and Chemical Sciences, University of L'Aquila.

In order to further characterize GO foil surface, the material was visualized by using the AFM technique. The AFM micrograph of GO foil (Figure 4) evidenced the presence of an easily recognizable 1 μM GO flake onto the surface.

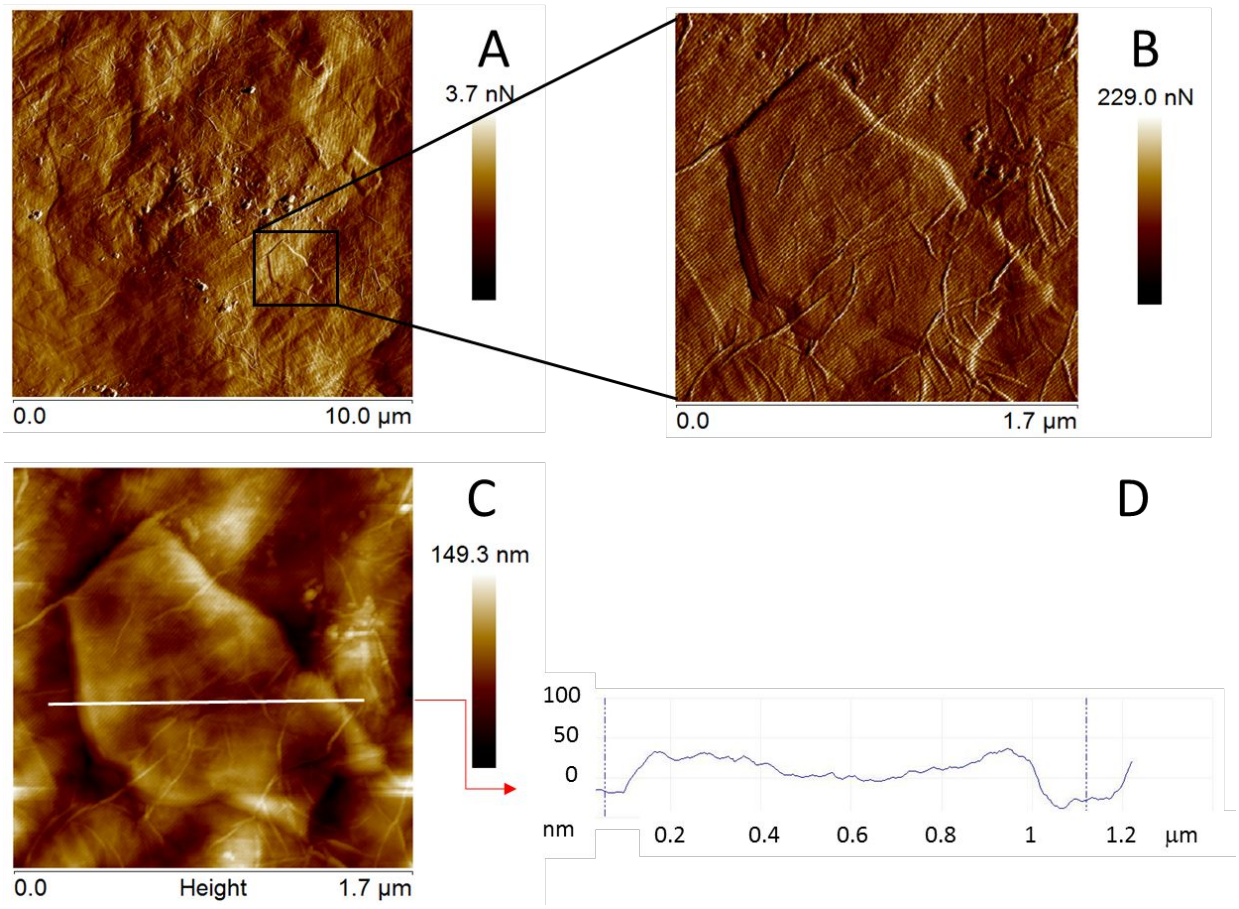

Figure 4. AFM images of GO foil obtained with Peak Force QNM reporting: A) peak force error (10 µm × 10 µm), B) inset of image A; C) and D) high of the inset B in planar and trace profile, respectively.

By exploiting the Peak Force quantitative Nanomechanical Mapping of the AFM instrument, a mapping of the adhesion, the dissipation energy and the deformation of the sample (Figure 5) as well as the determination, from the force curve on 38 random points, of the Young's modulus of the GO foil were obtained.

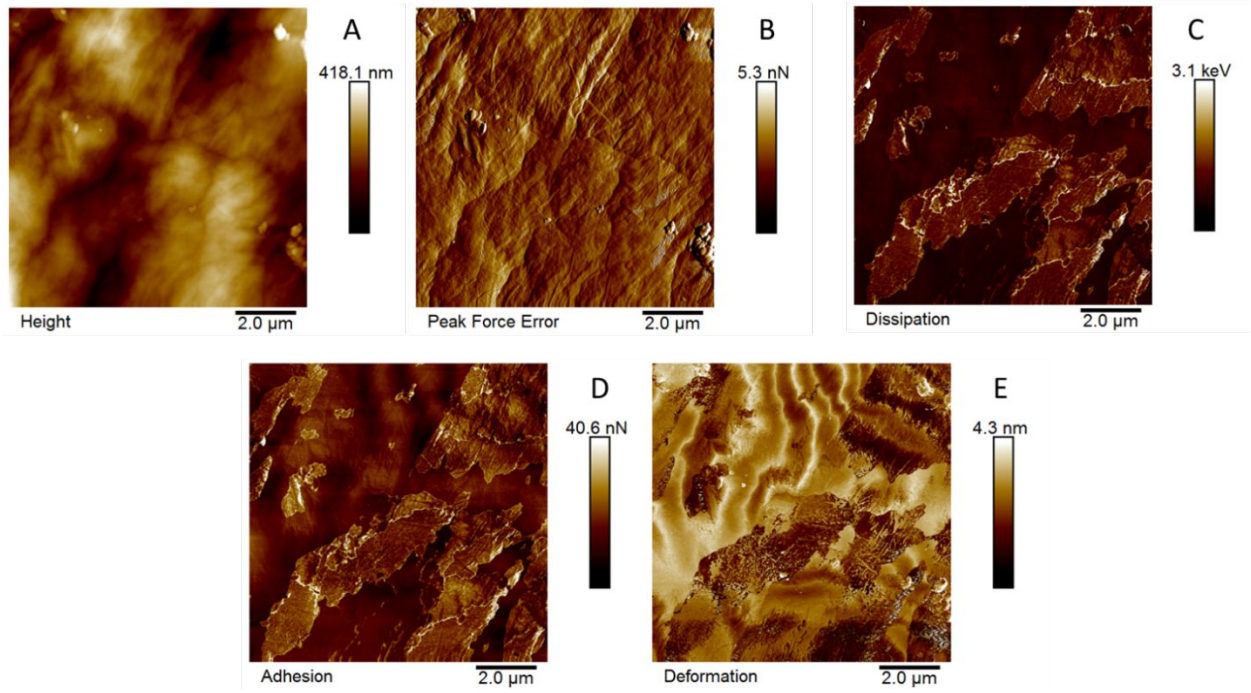

Figure 5. Peak Force QNM mapping of GO foil reporting: A) topographical mapping; B) peak force error; C) dissipation energy; D) adhesion and E) deformation of a 10 µm × 10 µm area.

3.2. SEM analyses of DPSCs cultured on GO foil. DPSCs morphology on control and GO foil was investigated by means of scansion electron microscopy after 3, 14 and 28 days of culture (Figure 6). After 3 days of culture DPSCs cultured on control surface have already formed a uniform layer (Figures 6A and 6B) whereas DPSCs cultured on GO foil were still adhering and organizing a collagen fibers network (Figures 6C and 6D). After 14 days of culture a similar trend with respect to 3 days was evidenced for DPSCs cultured on control surfaces (Figures 6E and 6F); on the contrary on GO foil a significant, well organized and markedly developed network of collagen fibers was clearly evidenced thus indicating that a consistent extracellular matrix was synthetized by DPSCs (Figures 6G and 6H). After 28 days of culture no significant differences could be detected between DPSC cultured on control and GO foil since cells formed a uniform layer throughout the surfaces (Figures 6I, 6J, 6K and 6L).

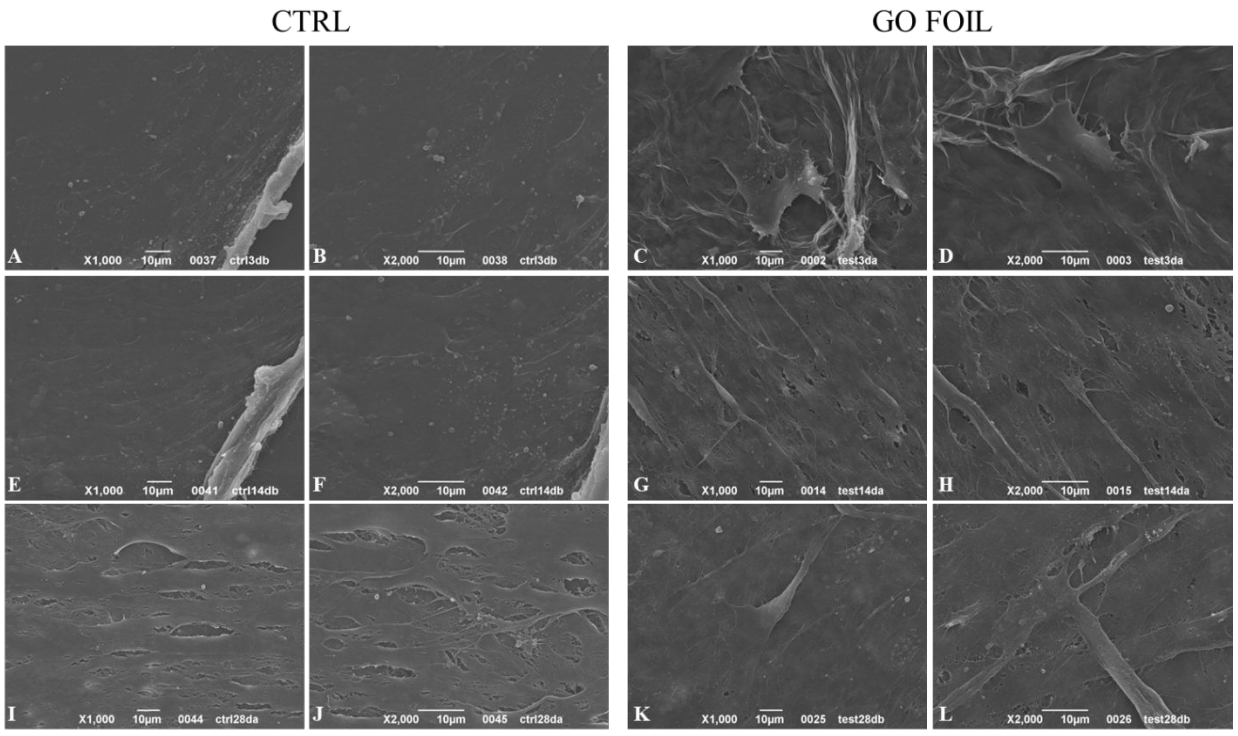

Figure 6. SEM images of DPSCs cultured on control and GO foil for 3, 14 and 21 days. Magnification 1000× and 2000×: A-D) 3 days of culture; E-H) 14 days of culture; I-L) 28 days of culture.

3.3. Viability measurements. DPSCs were cultured both on polystyrene surfaces (control) and on GO foil up to 28 days in the presence of an osteogenic differentiating medium; 3, 7, 14, 21 and 28 days of culture were established as experimental points. DPSCs viability was evaluated through Alamar Blue assay. A statistically significant increase in Alamar blue reduction percentage ($p<0.05$), and, as a consequence, in cell viability, was monitored on GO foil with respect to the control, after 3, 14 and 28 days of culture. Instead, no significant differences were observed after 7 days of culture (Figure 7A).

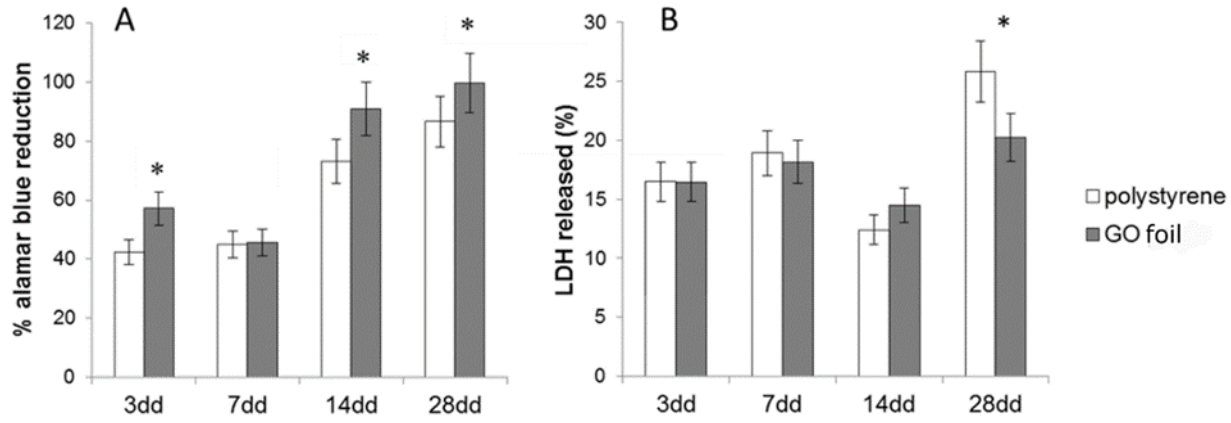

Figure 7. (A) Alamar blue test in DPSCs grown on polystyrene and GO foil for 3, 7, 14 and 28 days. The graph shows Alamar blue reduction percentage on polystyrene, used as the control, and GO foil. Data represented in the histograms are the mean (±SD) of three independent experiments. * days 3, 14 and 28: GO foil *vs.* polystyrene $p<0.05$. (B) LDH assay of DPSCs grown on polystyrene and GO foil for 3, 7, 14 and 28 days. LDH released is shown as percentage. Reported data are the average (±SD) of three independent experiments. *day 28: GO foil *vs.* polystyrene $p<0.01$.

Cytotoxicity was investigated by means of LDH test, as well. LDH test evidenced no statistically significant differences in cytotoxicity after 3, 7 and 14 days of culture between cells cultured on polystyrene and on GO foil. On the other hand a marked reduction ($p<0.01$) in cytotoxicity was recorded after 28 days of culture for DPSCs cultured on GO foil (Figure 7B).

3.4. Stem cells differentiation. DPSCs differentiation towards the osteoblastic lineage was investigated by measuring, through real-time RT-PCR, gene expression of osteogenic markers involved in different stages of differentiation. The expression of BMP2 gene, involved in the first stages of new matrix deposition, did not modify between cells cultured on two tested surfaces throughout the cell culture period (Figure 8A). After 7 days of culture, RUNX2, involved in

subsequent passages of the differentiation process, showed a marked increase ($p<0.01$) in DPSCs cultured on GO foil with respect to polystyrene-cultured ones, whereas no significant differences were revealed at the other experimental times (Figure 8B). Lastly, SP7, responsible of matrix mineralization, was investigated and its expression was significantly increased ($p<0.01$) after 14 days of DPSCs culture on GO foil with respect to DPSCs cultured on polystyrene surfaces. No significant differences of SP7 gene expression could be recorded at all other tested experimental times (Figure 8C). To confirm the data obtained by gene expression analysis, in cell supernatant of DPSCs committed to osteogenic differentiation, ALP activity was measured. An increase in ALP activity when DPSC are cultured on GO foils is recorded in all the experimental times with respect to DPSC cultured on polystyrene, with statistical significance after 3, 7 and 14 days of culture (Figure 9).

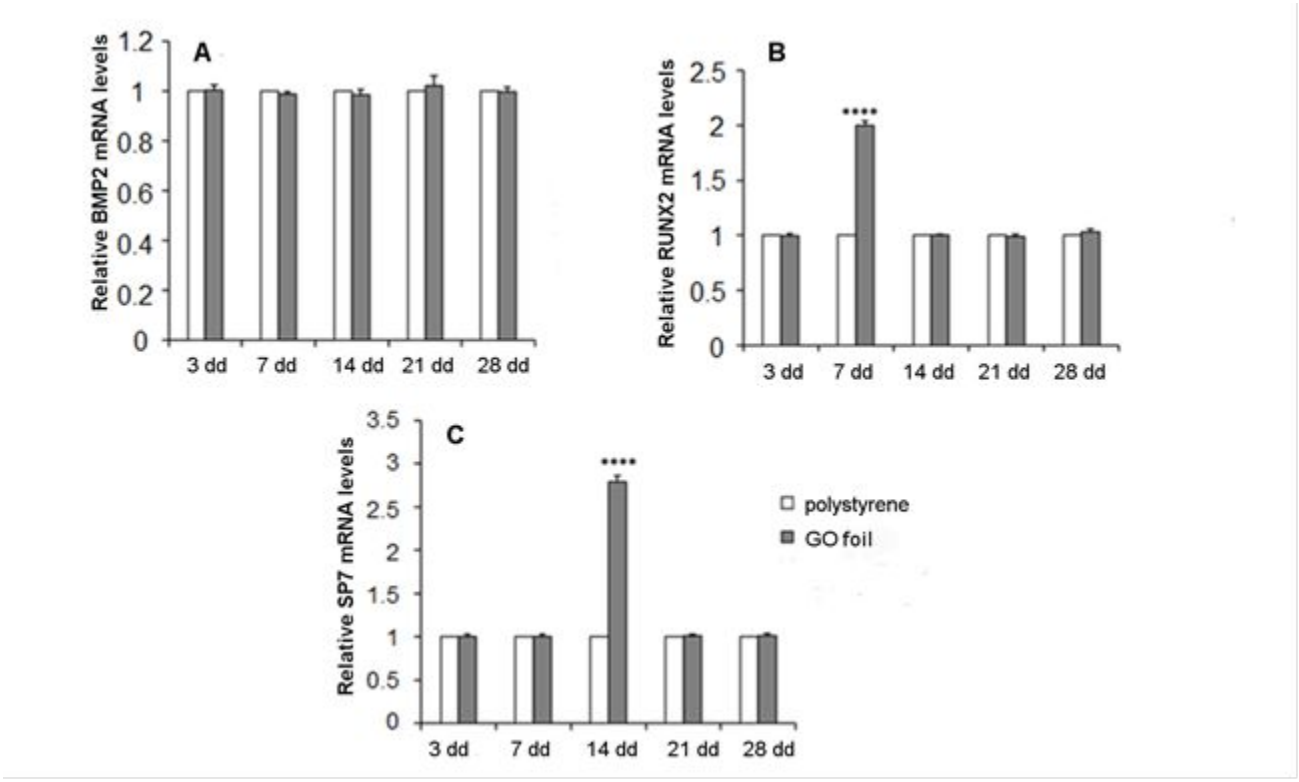

Figure 8. Relative gene expression of BMP2 (A), RUNX2 (B) and SP7 (C) in DPSCs grown on polystyrene and GO foil for 3, 7, 14, 21 and 28 days. Data are relative to control (calibrator sample, defined as 1). Reported data are the averages ± SD of three independent experiments. Y-axis, fold change. In (B): day 7 GO foil *vs.* polystyrene $p<0.0001$. In (C): day 14 GO foil *vs* polystyrene $p<0.0001$.

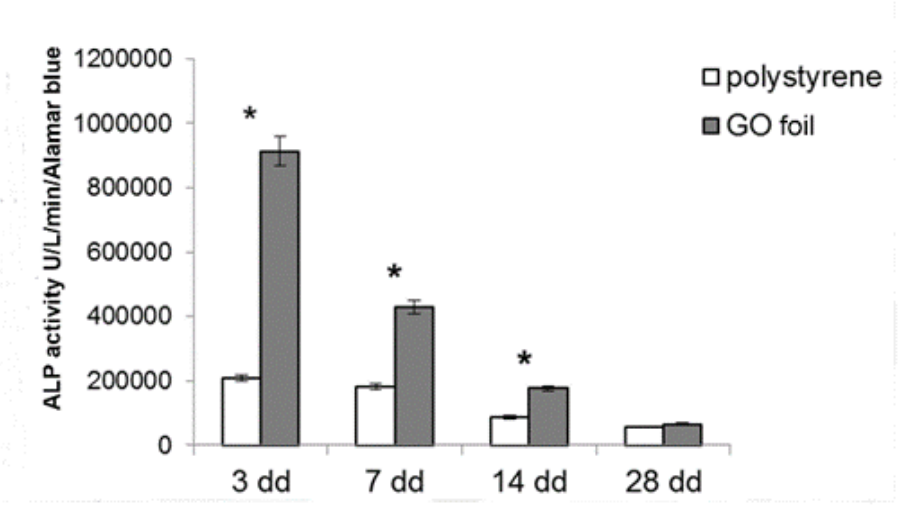

Figure 9. Alkaline phosphatase (ALP) activity in DPSCs cultured on polystyrene and GO foil for 3, 7, 14 and 28 days. Values represent the means ± SD. Bar graph showing the enzymatic activity of ALP (U/ml) normalized on Alamar blue values after 3, 7, 14 and 28 days of culture of DPSCs growth onto scaffolds. * days 3, 7 and 14: GO foil *vs.* polystyrene $p<0.05$.

4. DISCUSSION

Data obtained show that GO foil can be used as an efficient substrate in order to favour osteoblatic differentiation of DPSC. In particular, SEM analyses of bare GO foil evidence that the obtained foil has a layered structure and a thickness of 10 μm. The GO foil is stable in water

and PBS for at least one week and no leakage of GO in the solution could be monitored by spectrophotometric measurements during this period (see Supporting Information). This stability is due to the fact that reactive carboxylic acid and hydroxyl functional groups on individual GO flakes are involved in both i) hydrogen bond networks comprising water molecules within the interlayer cavities[10] and ii) crosslinks via divalent Ca^{2+} cations.[9] These bonds allow to create an almost homogeneous material in which each GO flake is bound to each other and does not disperse in aqueous solution. The formation of a cross-linked network is evidenced by the small interlayer distance of the majority of GO flakes in the foil (see Figure 3). Indeed only few, less interconnected, GO flakes, predominantly located onto the foil surface, show a marked gap among the neighboring ones. These flakes, slightly detached from the foil surface of ca. 40 nm, have been detected also by AFM (see Figure 4D), whereas the remaining ones form a seamless piece. The GO foil demonstrates to be prevailingly elastic in nature with low dissipation energy. Adhesion for the tip is confined to a few superficial GO flakes (Figure 5D). Indeed, the structure of GO foil is not perfectly homogeneous because, due to the different water flow and evaporation degree across the foil during the filtration step, the arrangement of the top layers is less ordered than that of the bottom layers. This means that GO foil contains voids and is assimilable to a porous material. In agreement with this evidence, it has been previously demonstrated that the Young's modulus of GO foils produced without the addition of calcium ions depends on the thickness of the paper with thicker papers, characterized by a marked difference of water flow during preparation among the top and bottom layers, being much less stiff[26] than thinner ones. The deformation, i.e. the penetration of the tip into the surface at the peak force, is relatively low and depends on the stiffness of the GO foil. The measured Young's elastic modulus, 2.3±0.8 GPa, has a value in between the stiffness of osteocalcin-rich osteoid matrix (27.0 ± 10 kPa)[27] and that

of the mean value of Young's modulus in trabecular bone in the human mandible (25.0 ± 5.6 GPa).[28] By considering that mechanotransduction effect has been recognized to regulate stem cell differentiation,[14] mesenchymal stem cells sense[27] matrix elasticity and preferentially differentiate depending of the stiffness of the substrate - with soft matrices (E = 0.1-1 kPa) that mimic brain being neurogenic, and stiffer matrices proving to be osteogenic - this value appears proper to favor expression of an osteogenic lineage. Moreover, it is very similar to that of polyethylene (1.5-2 GPa) or polystyrene (3-3.5 GPa) substrates which have been previously demonstrated to be ideal substrates for the growth of stem cells.

DPSCs viability, evaluated by means of Alamar blue staining, significantly increases throughout the culture period when DPSCs are cultured on GO foil with respect to cells grown on polystyrene, indicating a favorable interaction of DPSCs with the GO foil.

In addition, the Lactate Dehydrogenase test demonstrates that the obtained GO foil is not cytotoxic for the cells and actually at 28 days GO foil proved to be less cytotoxic than polystyrene itself.

Despite we did not investigate in detail the reasons for such an effect, we think that different features of the GO foil contribute to it. First of all, GO foil - thanks to graphene π-electron clouds and carboxylic and hydroxyl groups that render it capable of interacting, respectively, via hydrophobic and electrostatic interactions with different proteins - favors protein adsorption,[29,30] an essential issue for regulating cell functions and mediate cell adhesion and morphology.[31,32] This effect, associated to a Young's modulus similar to that of polystyrene, could promote osteogenic differentiation.

Secondly, Lee at al.[29] have previously showed that GO substrates concentrate osteogenic induction media on their surface. In our experiments DPSCs were seeded and then cultured both on cell culture-treated polystyrene surfaces (control) and on GO foils up to 28 days in the presence of an osteogenic differentiating medium. The resulting increase of the concentration of osteogenic induction molecules could promote gene expression of osteogenic differentiation markers.

In the present work we measured the gene expression of three osteogenic factors, with different roles and involved in different moments of the osteoblastic differentiation. BMP2 is an early marker of the osteogenic differentiation whose signaling pathway is fundamental to initiate osteoblast differentiation.[33] BMP2, in turn, promotes, the expression of RUNX2 transcription factor mRNA.[34] RUNX2 mediates the transformation from progenitor cells to preosteoblasts, whereas, SP7, a second transcription factor considered a late marker of the osteogenic process, directs the preosteobasts to immature osteoblasts allowing the mineralization of the already synthetized matrix.[35] Our results were very promising as they clearly show that only for DPSCs cultured on GO foils the molecular signaling leading to a final osteogenic differentiation is triggered, as demonstrated by both RUNX2 increase after 7 days and SP7 increase recorded after 14 days of culture. These findings markedly evidence that the osteogenic differentiation starts and progresses earlier and better when DPSCs are cultured on GO foil with respect to control. Regarding BMP2 gene expression, being a very early marker of the process, it is likely that its expression raised up before 3 days of culture.

These evidences are confirmed by SEM analyses of DPSCs cultured on GO foils (see Figure 6). As a matter of fact only at the earliest investigated times (i.e. 3 and 14 days) the synthesis of extracellular matrix and the relevant formation of a network of collagen fibers were promoted by

the presence of GO foil. At 28 days cells cultured on polystyrene and GO foils formed in both cases a uniform layer throughout the surfaces.

Moreover, the activity of ALP, which is strictly related to early bone matrix deposition stages,[13,36] clearly evidences a promotion of DPSC differentiation along all the experimental period when they are cultured on GO foils instead of polystyrene surfaces.

Last but not least, the chelated calcium ions present in the interconnected network of GO flakes may favorably contribute to osteogenic differentiation of DPSCs. Indeed, it has been demonstrated that the presence of calcium ions on hydrothermally treated titanium substrate favors the adhesion, increases the growth rate of osteoblast like cells, such as MC3T3-E1, and effectively contributes to the precipitation of bone-like apatite on the titanium during immersion in simulated body fluid, with respect to pure titanium substrate.[37] Similarly titanium implant surfaces, modified with calcium ions via sonication, have been recently demonstrated to stimulate osteoblastic cell attachment, proliferation and differentiation.[38] Indeed, calcium ions are included in GO foils and therefore they are available for cell absorption.

These data clearly underline the GO foils capability to promote a faster and better DPSCs differentiation with respect to polystyrene substrate, thus representing a promising preliminary result for future *in vivo* evaluations aiming at providing an improvement of tissue engineering and oral implants healing.

5. CONCLUSIONS

The prepared GO foils demonstrate to be characterized by closely interconnected GO flakes as evinced by SEM and AFM analyses. In particular GO flakes form a continuous and stable surface whose Young's modulus, measured via AFM Peak Force QNM in air, is 2.3 GPa that is

comparable with that of polystyrene and much lower than that of reduced 2D graphene oxide sheet (0.25 TPa).[39] Indeed, the obtained GO foil, organized in a 3D porous structure, is less stiff than pure bidimensional GO flakes. This value of elastic modulus is comparable to the values obtained for GO enriched polymer hybrids whose increase of Young's modulus, with respect to the pure polymer, has been previously ascribed to the hydrogen bonding formed between the oxygen-containing moieties attached to the graphene surface and the surrounding polymer.[40] Therefore the observed Young's modulus in the synthesized GO foil is the result of hydrogen bond networks comprising water molecules and GO sheets as well as the crosslinks via divalent Ca^{2+} cations. The GO foil demonstrates to favor DSPCs viability with respect to polystyrene and no evidence of toxic effects has been detected. Transcription factors associated with osteogenic differentiation (RUNX2) or responsible for triggering bone matrix mineralization (SP7) appear to be significantly increased, with respect to the control, indicating that GO foil could be able to promote a faster DPSCs differentiation. SEM analyses evidence an early promotion of the synthesis of extracellular matrix and the formation of collagen fiber network as compared to DPSCs cultured on control polystyrene. These effects may be ascribed to the structure of the GO foil, characterized by interconnected layers of GO and voids resembling porous bone and a relatively intermediate value of Young's modulus. Furthermore they are presumably connected with the capacity of GO to favor protein absorption, to concentrate osteogenic induction molecules as well as chelated calcium ions in the interconnected network of GO flakes.

Electronic Supporting Information

Supporting Information. Stability measurements of graphene foil in water. This material is available free of charge via the Internet at http://pubs.acs.org.

AUTHOR INFORMATION

Corresponding Author

*Antonella Fontana, email: antonella.fontana@unich.it.

ACKNOWLEDGMENT

We acknowledge prof. Maurizio Passacantando (Department of Physical and Chemical Sciences, University of L'Aquila, Coppito, L'Aquila, Italy) for SEM measurements. We thank MIUR and University "G. d'Annunzio" (FAR 2017 and FAR 2018) for financial support.

ABBREVIATIONS

GO, graphene oxide; DSPCs, Dental Pulp Stem Cells; RUNX2, Runt-related transcription factor 2 associated with osteogenic differentiation; SP7, transcription factors responsible for triggering bone matrix mineralization; $CaCl_2$, Calcium Chloride; PBS, Phosphate buffer; AFM, Atomic Force Microscopy; SEM, Scanning Electron Microscopy; FBS, Fetal Bovine Serum; α-MEM, Minimum Essential Medium Eagle - Alpha Modifications; DM, differentiation medium; LDH, Lactate Dehydrogenase; RT, Reverse transcription; real-time RT-PCR, real-time-polymerase chain reaction; BMP2, bone morphogenic protein 2; GAPDH, Glyceraldehyde-3-phosphate dehydrogenase; QNM, Quantitative Nanomechanical property Mapping.

REFERENCES

(1) Geim, A. K.; Novoselov, K. S. The Rise of Graphene. *Nat. Mater.* **2007**, *6*, 183−191.

(2) Novoselov, K. S.; Geim, A. K.; Morozov, S. V.; Jiang, D.; Zhang, Y.; Dubonos, S. V.; Grigorieva, I. V.; Firsov, A. A. Electric Field Effect in Atomically Thin Carbon Films. *Science* **2004**, *306*, 666−669.

(3) Brink, J v. d. From Strength to Strength. Nat. Nanotechnol. **2007**, *2*, 199−201.

(4) Dreyer, D. R.; Park, S.; Bielawski, C. W.; Ruoff, R. S. The Chemistry of Graphene Oxide. *Chem. Soc. Rev.* **2010**, 39, 228−240.

(5) Ettorre, V.; De Marco, P.; Zara, S.; Perrotti, V.; Scarano, A.; Di Crescenzo, A.; Petrini, M.; Hadad, C.; Bosco, D.; Zavan, B.; Valbonetti, L.; Spoto, G.; Iezzi, G.; Piattelli, A.; Cataldi, A.; Fontana, A. In Vitro and in Vivo Characterization of Graphene Oxide Coated Porcine Bone Granules. *Carbon* **2016**, *103*, 291−298.

(6) Stankovich, S.; Piner, R.; Nguyen, S. T.; Ruoff, R. S. Synthesis an Exfoliation of Isocyanate-Treated Graphene Oxide Nanoplatelet. *Carbon* **2006**, *44*, 3342−3347.

(7) Lerf, A.; He, H.; Forster, M.; Klinowski, J. Structure of Graphite Oxide Revisited. *J. Phys. Chem. B* **1998**, *102*, 4477−4482.

(8) Zhu, Y.; Murali, S.; Cai, W.; Li, X.; Suk, J. W.; Potts, J. R.; Ruoff, R. S. Graphene and Graphene Oxide: Synthesis, Properties, and Applications. *Adv. Mater.* **2010**, 22, 3906−3924.

(9) Park, S.; Lee, K.-S.; Bozoklu, G.; Cai, W.; Nguyen, S. T.; Ruoff, R S. Graphene Oxide Papers Modified by Divalent Ions—Enhancing Mechanical Properties via Chemical Cross-Linking. *ACS Nano* **2008**, *2*, 572−578.

(10) Medhekar, N. V.; Ramasubramaniam, A.; Ruoff, R. S.; Shenoy, V. B. Hydrogen Bond Networks in Graphene Oxide Composite Paper: Structure and Mechanical Properties, *ACS Nano* **2010**, *4*, 2300–2306.

(11) Kim, T. H.; Shah, S.; Yang, L. T.; Yin, P. T.; Hossain, M. K.; Conley, B.; Choi, J. W.; Lee, K. B. Controlling Differentiation of Adipose-Derived Stem Cells Using Combinatorial Graphene Hybrid-Pattern Arrays. *ACS Nano* **2015**, *9*, 3780−3790.

(12) Jung, H. S.; Lee, T.; Kwon, I. K.; Kim, H. S.; Hahn, S. K.; Lee, C. S. Surface Modification of Multipass Caliber-Rolled Ti Alloy with Dexamethasone-Loaded Graphene for Dental Applications. *ACS Appl. Mater. Interfaces* **2015**, *7*, 9598−9607.

(13) Luo, J.; Zhang, X.; Machuki, J. O.; Dai, C.; Li, Y.; Guo, K.; Gao, F. Three-Dimensionally N-Doped Graphene−Hydroxyapatite/Agarose as an Osteoinductive Scaffold for Enhancing Bone Regeneration. *ACS Appl. Bio Mater*, Ahead of print. DOI: 10.1021/acsabm.8b00599.

(14) Tatavarty, R.; Ding, H.; Lu, G.; Robert J. Taylor, R. J.; Bi, X. Synergistic Acceleration in the Osteogenesis of Human Mesenchymal Stem Cells by Graphene Oxide–Calcium Phosphate Nanocomposites. *Chem. Commun.* **2014**, 50, 8484-8487.

(15) Bernabò, N.; Fontana, A.; Ramal Sanchez, M.; Valbonetti, L.; Capacchietti, G.; Zappacosta, R.; Greco, L.; Marchisio, M.; Lanuti, P.; Ercolino, E.; Barboni, B. Graphene Oxide Affects in Vitro Fertilization Outcome by Interacting with Sperm Membrane in an Animal Model, *Carbon* **2018**, *129*, 428-437.

(16) Di Giulio, M.; Zappacosta, R.; Di Lodovico, S.; Di Campli, E.; Siani, G.; Fontana, A.; Cellini, L. Antimicrobial and Antibiofilm Efficacy of Graphene Oxide Against Chronic Wound Microorganisms, *Antimicrob. Agents Chemother*. **2018**, *62*, 00547-18, 1-9. DOI: 10.1128/AAC.00547-18.

(17) Zappacosta, R.; Di Giulio, M.; Ettorre, V.; Bosco, D.; Hadad, C.; Siani, G.; Di Bartolomeo, S.; Cataldi, A.; Cellini, L; Fontana, A. Liposome-Induced Exfoliation of Graphite to Few_Layer Graphene Dispersion with Antibacterial Activity, *J. Mater. Chem. B*. **2015**, *3*, 6520-6527.

(18) Elkhenany, H.; Amelse, L.; Lafont, A.; Bourdo, S.; Caldwell, M.; Neilsen, N.; Dervishi, E.; Derek, O.; Biris, A. S.; Anderson, D.; Dhar, M. Graphene Supports in Vitro Proliferation and Osteogenic Differentiation of Goat Adult Mesenchymal Stem Cells: Potential for Bone Tissue Engineering. *J. Appl. Toxicol*. **2015**, *35*, 367–374.

(19) Dikin, D. A.; Stankovich, S.; Zimney, E. J.; Piner, R. D.; Dommett, Geoffrey H. B.; Evmenenko, G.; Nguyen, S. T. ; Ruoff, R. S. Preparation and Characterization of Graphene Oxide Paper. *Nature* **2007**, *448*, 457−460.

(20) Rosa, V.; Xie, H.; Dubey, N.; Madanagopal, T. T.; Rajan, S. S.; Morin, J. L.; Islam, I.; Castro Neto, A. H. Graphene Oxide-Based Substrate: Physical and Surface Characterization, Cytocompatibility and Differentiation Potential of Dental Pulp Stem Cells, *Dent. Mater*. **2016**, *32*, 1019-1025.

(21) Tatavarty, R.; Ding, H.; Lu, G.; Taylor, R. J.; Bi, X. Synergistic Acceleration in the Osteogenesis of Human Mesenchymal Stem Cells by Graphene Oxide-Calcium Phosphate Nanocomposites, *Chem. Commun*, **2014**, *50*, 8484-8487.

(22) Xie, H.; Cao, T.; Rodríguez-Lozano, F. J.; Luong-Vanc, E. K.; Rosa, V. Graphene for the Development of the Next-Generation of Biocomposites for Dental and Medical Applications, *Dent. Mater.* **2017**, *33*, 765-774.

(23) Radunovic, M.; De Colli, M.; De Marco, P.; Di Nisio, C.; Fontana, A.; Piattelli, A.; Cataldi, A.; Zara, S. Graphene Oxide Enrichment of Collagen Membranes Improves DPSCs Differentiation and Controls Inflammation Occurrence, *J. Biomed. Mater. Res. A* **2017**, *105*, 2312-2320.

(24) De Marco, P.; Zara, S.; De Colli, M.; Radunovic, M.; Lazović, V.; Ettorre, V.; Di Crescenzo, A.; Piattelli, A.; Cataldi, A.; Fontana, A. Graphene Oxide Improves the Biocompatibility of Collagen Membranes in an in Vitro Model of Human Primary Gingival Fibroblasts, *Biomed. Mater.* **2017**, 12, 055005.

(25) Han, D.-D.; Zhang, Y.-L.; Liu, Y.; Liu, Y.-Q.; Jiang, H.-B.; Han, B.; Fu, X.-Y.; Ding, H.; Xu H-L, Sun H-B. Bioinspired Graphene Actuators Prepared by Unilateral UV Irradiation of Graphene Oxide Papers. *Adv. Funct. Mater*. **2015**, *25*, 4548−4557.

(26) Gong, T.; Van Lam, Do.; Liu, R.; Won, S.; Hwangbo, Y.; Kwon, S.; Kim, J.; Sun, K.; Kim, J.-H.; Lee, A.-M.; Lee, C. Thickness Dependence of the Mechanical Properties of Free Standing Graphene Oxide Papers, *Adv. Funct. Mater*. **2015**, *25*, 3756−3763.

(27) Engler,A. J.; Sen, S.; Sweeney, H. L.; Discher, D. E. Matrix Elasticity Directs Stem Cell Lineage Specification, *Cell* **2006**, *126*, 677−689.

(28) Nomura, T.; Katz, J. L.; Powers, M. P.; Saito, C. A Micromechanical Elastic Property Study of Trabecular Bone in the Human Mandible, *J. Mater. Sci: Mater. Med*. **2007**, *18*, 629−633.

(29) Lee, W. C.; Lim, C. H. Y. X.; Shi, H.; Tang, L. A. L.; Wang, Y.; Lim, C. T.; Loh, K. P. Origin of Enhanced Stem Cell Growth and Differentiation on Graphene and Graphene Oxide. *ACS Nano* **2011**, *5*, 7334−7341.

(30) Portone, A.; Moffa, M.; Gardin, C.; Ferroni, L.; Tatullo, M.; Fabbri, F.; Persano, L.; Piattelli, A.; Zavan, B.; Pisignano, D. Lineage-Specific Commitment of Stem Cells with Organic and Graphene Oxide–Functionalized Nanofibers. *Adv. Funct. Mater.* **2018**, Ahead of Print. DOI: 10.1002/adfm.201806694.

(31) Woo, K. M.; Seo, J.; Zhang, R. Y.; Ma, P. X. Suppression of Apoptosis by Enhanced Protein Adsorption on Polymer/Hydroxyapatite Composite Scaffolds. *Biomaterials* **2007**, *28*, 2622−2630.

(32) Woo, K. M.; Chen, V. J.; Ma, P. X. Nano-Fibrous Scaffolding Architecture Selectively Enhances Protein Adsorption Contributing to Cell Attachment. *J. Biomed. Mater. Res., Part A* **2003**, *67A*, 531−537.

(33) Liu, H.; Zhang, R.; Chen, D.; Oyajobi, B.O.; Zhao, M. Functional Redundancy of Type II BMP Receptor and Type IIB Activin Receptor in BMP2-Induced Osteoblast Differentiation. *J. Cell Physiol.* **2012,** *227*, 952–963.

(34) Lee, M. H.; Kim, Y.J.; Kim, H. J.; Park, H. D.; Kang, A. R.; Kyung, H. M,; Sung, J. H.; Wozney, J. M.; Kim, H. J.; Ryoo, H. M.. BMP-2-Induced Runx2 Expression is Mediated by Dlx5, and TGF-Beta 1 Opposes the BMP-2-Induced Osteoblast Differentiation by Suppression of Dlx5 Expression. *J. Biol. Chem*. **2003,** *278*, 34387-34394.

(35) Komori, T. Regulation of Osteoblast Differentiation by Transcription Factors. *J. Cell Biochem.* **2006,** *99*, 1233-1239.

(36) Lin, J.; Shao, J.; Juan, L.; Yu, W.; Song, X.; Liu, P.; Weng, W.; Xu, J.; Mehl, C. Enhancing Bone Regeneration by Combining Mesenchymal Stem Cell Sheets with β-TCP/COL-I Scaffolds *J. Biomed. Mater. Res. B Appl. Biomater*. **2017**, *106(5)*, 2037-2045. DOI: 10.1002/jbm.b.34003.

(37) Nakagawa, M.; Zhang, L.; Udoh, K.; Matsuya, S.; K. Ishikawa, K. Effects of Hydrothermal Treatment with $CaCl_2$ Solution on Surface Property and Cell Response of Titanium Implants. *J. Mater. Sci.-Mater. Med.* **2005**, *16*, 985−991.

(38) Anitua, E.; Piñasa, L.; Murias, A.; Prado, R.; Tejero, R. Effects of Calcium Ions on Titanium Surfaces for Bone Regeneration. *Colloid Surf. B-Biointerfaces* **2015**, *130*, 173–181.

(39) Gómez-Navarro, C.; Burghard, M.; Kern, K. Elastic Properties of Chemically Derived Single Graphene Sheets, *Nano Lett.* **2008**, *8*, 2045−2049.

(40) Liang, J.; Huang, Y.; Zhang, L.; Wang, Y.; Ma, Y.; Guo, T.; Chen, Y. Molecular-Level Dispersion of Graphene into Poly(vinyl Alcohol) and Effective Reinforcement of their Nanocomposites. *Adv. Funct. Mater.* **2009**, *19*, 2297−2302.

Graphical Abstract